Drug Design, Development and Therapy

Dovepress
open access to scientific and medical research

Open Access Full Text Article

ORIGINAL RESEARCH

Tackling Microbial Resistance with Isatin-Decorated Thiazole Derivatives: Design, Synthesis, and in vitro Evaluation of Antimicrobial and Antibiofilm Activity

Refaie M Kassab[1], Sami A Al-Hussain[2], Nooran S Elleboudy[3], Amgad Albohy[4], Magdi EA Zaki[2], Khaled AM Abouzid[5,6], Zeinab A Muhammad[7]

[1]Department of Chemistry, Faculty of Science, Cairo University, Giza, 12613, Egypt; [2]Department of Chemistry, Faculty of Science, Imam Mohammad Ibn Saud Islamic University (IMSIU), Riyadh, 11623, Saudi Arabia; [3]Department of Microbiology and Immunology, The Faculty of Pharmacy, Ain Shams University, Cairo, 11566, Egypt; [4]Department of Pharmaceutical Chemistry, Faculty of Pharmacy, The British University in Egypt (BUE), Cairo, 11837, Egypt; [5]Department of Pharmaceutical Chemistry, Faculty of Pharmacy, Ain Shams University, Cairo, 11566, Egypt; [6]Department of Organic and Medicinal Chemistry, Faculty of Pharmacy, University of Sadat City, Sadat City, Egypt; [7]Department of Organic Chemistry, National Organization for Drug Control and Research (NODCAR), Giza, 12311, Egypt

Correspondence: Refaie M Kassab, Department of Chemistry, Faculty of Science, Cairo University, Giza, 12613, Egypt, Tel +20101-336-2594, Fax +20-25685799, Email rkassab@sci.cu.edu.eg; Sami A Al-Hussain, Department of Chemistry, Faculty of Science, Imam Mohammad Ibn Saud Islamic University (IMSIU), Riyadh, 11623, Saudi Arabia, Email sahussain@imamu.edu.sa

Introduction: Antibiotic resistance is a global threat that has been increasing recently, especially with antibiotic overuse and misuse. The search for new antibiotics is becoming more and more indispensable.

Methods: Design and synthesis of isatin derivatives as surrogates of SB-239629, a bacterial tyrosine-tRNA synthetases (TyrRS) inhibitor. The newly synthesized compounds were screened for their antimicrobial and antibiofilm activities. Docking studies were used to investigate potential binding modes of these compounds with TyrRS.

Results and Discussion: Newly synthesized isatin-decorated thiazole derivatives (7b, 7d, and 14b) have shown potent antimicrobial activities against *E. coli*, a representative of gram-negative bacteria. Also, 7f showed the best activity against Methicillin Resistant *Staphylococcus aureus* (MRSA). In addition, 7h and 11f were found to have antifungal activities against *Candida albicans* equivalent to that of the reference Nystatin. All the new isatin derivatives with antimicrobial activities were found to exhibit strong biofilm distortion effects at half their minimum inhibitory concentrations (MIC). Moreover, thiazole derivatives 11a-f showed promising biofilm formation inhibition. Finally, molecular docking studies were used to investigate possible binding modes of target compounds with *S. aureus* and *E. coli* TyrRS.

Conclusion: The novel isatin-decorated thiazole derivatives show strong antimicrobial and antifungal activities with potential action on TyrRS.

Keywords: 5-bromoisatin, thiosemicarbazone, hydrazonoyl chlorides, thiazoles, Tyrosyl-tRNA synthetases (TyrRS) inhibitors, antimicrobial, molecular docking, MRSA, antibiofilm

Introduction

Antimicrobial resistance is a seriously pressing international health concern.[1] If antimicrobial resistance keeps growing at the current rate, by the year 2050, superbugs could potentially be responsible for over 10 million annual deaths.[2] To hinder this ever-growing threat, health-care authorities work eagerly to reduce the abuse of antibiotics, as well as develop new prototypes with more potent antimicrobial activities. Among the well-known resistant and virulent bacterial strains are the Methicillin-Resistant *S. aureus* (MRSA). MRSA is *S. aureus* isolates with oxacillin minimum inhibitory concentrations (MIC) of 4 μg/mL or more. MRSA causes most nosocomial infections with challenging management and high mortality levels.[3] To generate new chemical entities (NCE) with antimicrobial activity against resistant strains we need to investigate new and/or old bacterial targets. Among the proven druggable antibacterial targets against MRSA

Received: 20 March 2022
Accepted: 2 July 2022
Published: 25 August 2022

and others are the aminoacyl-tRNA synthetases which play an important role in protein synthesis.[4] These groups of enzymes are required for the formation of aminoacyl-tRNA which is required during genetic code translation.[5] The isoleucyl-tRNA synthetases inhibitor, mupirocin, is a well-known antibacterial agent that proves this concept.[6] Tyrosyl-tRNA synthetase (TyrRS) was among the first aminoacyl-tRNA synthetases to be studied on different levels.[7,8] Several bacterial TyrRS are crystalized with known inhibitors. Examples of these include *Escherichia coli* TyrRS complexed with 5'-O-[N-(L-tyrosyl)sulfamoyl]adenosine (Tyr-AMS, I) (PDB ID: 1VBM) and *S. aureus* TyrRS in complex with SB-239629 (II) (PDB ID: 1JIJ) (Figure 1).

Another factor that contributes to the virulence of bacterial resistance is the formation of biofilms. Biofilms are multi-layered bacterial populations surrounded by a polysaccharide matrix. A considerable proportion of bacterial pathogens produce those biofilms as a virulence factor for adhesion to surfaces and shielding from antimicrobials. Biofilms are considered a serious health problem, responsible for over 80% of withstanding microbial infections.[9] As a result, and based on the major role biofilms play in the spread of infections and the emergence of resistance, there is an urgent need for the discovery of new chemotherapeutic agents that interfere with biofilm formation and/or disrupt preformed ones.[10]

Recently, we examined the intrinsic reactivity of hydrazonoyl chlorides towards thiosemicarbazones to construct various thiazole derivatives.[11,12]

In this report, and in continuation of our previous work on the synthesis of various bioactive heterocyclic compounds,[13–15] we present the design of some novel isatin-decorated thiazole derivatives. Isatin is a very important scaffold that could be easily decorated chemically to produce versatile compounds with different biological activities. For example, isatin derivatives were found to exert an anticancer effect through multiple mechanisms that include histone deacetylase (HDAC) inhibition,[16] carbonic

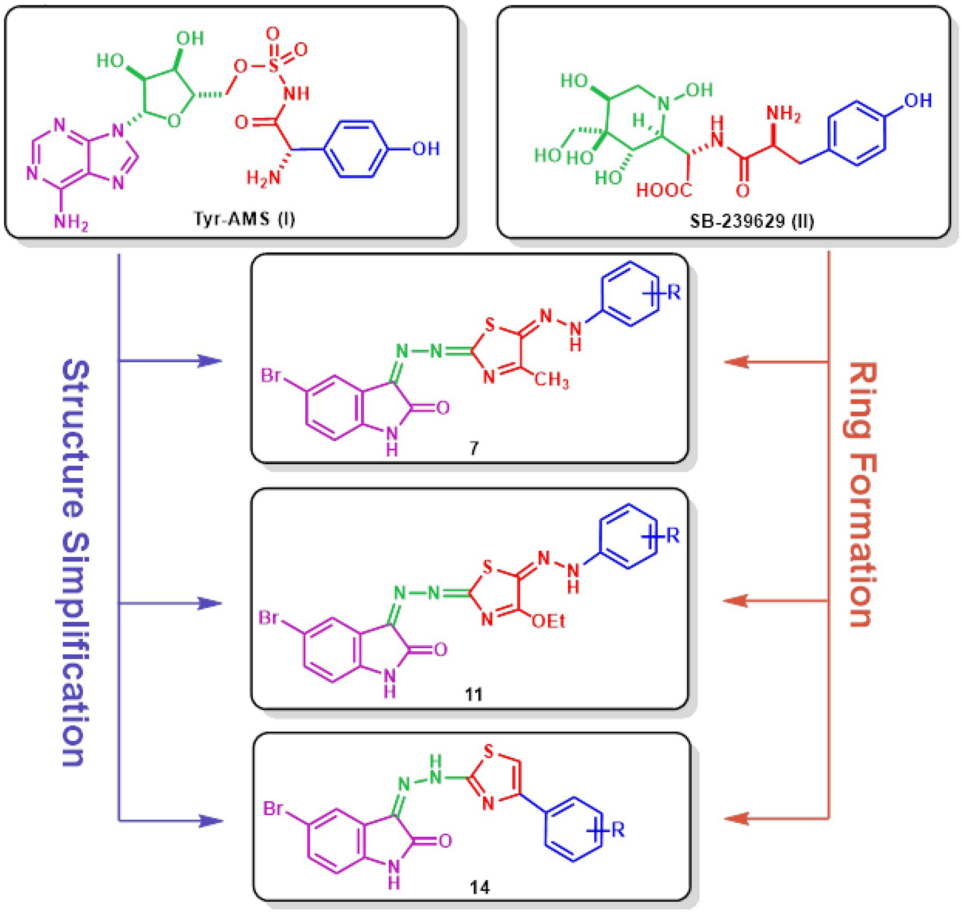

Figure 1 Design of target compounds based on Tyr-AMS (I) and SB-239629 (II) structures which are co-crystalized ligands inhibiting *Staphylococcus aureus* and *Escherichia coli* TyrRS.

anhydrase inhibition,[17] epidermal growth factor receptor - tyrosine kinase (EGFR-TK) inhibition[18] and tubulin inhibition.[19] Furthermore, isatins were also found to exert anti-bacterial, anti-diabetic, and anti-convulsant activities.[20] Here, our design was based on the structures of Tyr-AMS (I) and SB-239629 (II) Figure 1. The purine ring of Tyr-AMS (purple color) was substituted with the isatin ring in our target compounds. Also, sugar in both leads (green color) was simplified to a hydrazine moiety. In addition, tyrosine side chain (blue color) was maintained as a substituted phenyl ring in the designed compounds. Finally, the linker in lead structures (red color) was cyclized to form a thiazole ring. These novel isatin-based compounds were screened for their probable antimicrobial effect on *E. coli*, MRSA and *C. albicans* as well as their potential as anti-biofilm formation agents. The newly synthesized isatin-based thiazole derivatives were also subjected to molecular docking evaluation considering them as mimics for SB-239629 and Tyr-AMS.

Methods

Chemistry

Melting points were determined on a Gallenkamp apparatus and are uncorrected. IR spectra were recorded in potassium bromide using Pye-Unicam SP300 spectrophotometer. ^{1}H and ^{13}C NMR spectra were recorded in deuterated DMSO-d_6 using a Varian Gemini 300 NMR spectrometer (300 MHz for ^{1}H NMR and 75 MHz for ^{13}C NMR) and the chemical shifts were related to that of the solvent DMSO-d_6. Mass spectra were recorded on a GCMS-Q1000-EX Shimadzu and GCMS 5988-A HP spectrometers, the ionizing voltage was 70 eV. Elemental analyses of the products were carried out at the Microanalytical Centre of Cairo University, Giza, Egypt. The biological evaluation of the products was carried out at the Department of Microbiology and Immunology, The Faculty of Pharmacy, Ain Shams University, Cairo, Egypt. Compounds 4a-h were prepared as previously reported.[21] Compounds 8a-f were prepared as previously reported.[22]

General Procedure for the Synthesis of Hydrazonoyl Chloride Derivatives 4a-h and 8a-f

A solution of 20 mmol of the corresponding aromatic amine in 10 mL of dilute (1:1) hydrochloric acid was cooled to 0°C, and a solution of 1.52 g (22 mmol) of sodium nitrite in 10 mL of water was added dropwise while stirring and the mixture was further stirred for 15 minutes at 0°C. The resulting solution of diazonium salt was added dropwise to a cold solution of 2.7 g (20 mmol) of 3-chloro-2,4-pentanedione (for compounds 4a-h) or 3.3 g (20 mmol) of ethyl 2-chloro-4-oxobutanoate (for compounds 8a-f) and 2.46 g (30 mmol) of sodium acetate in 50 mL of aqueous ethanol (9:1). The reaction was stirred for an additional 4h while being allowed to warm up to room temperature. The mixture was then poured onto 500 mL of water and the formed precipitate was filtered, air dried, and recrystallized from ethanol.

(Z)-2-(5-bromo-2-oxoindolin-3-ylidene)hydrazine-1-carbothioamide (3) was synthesized according to a reported procedure[23]

Yellow solid, 90% yield; mp. 279–280 °C, (lit 270–271 °C) (Dioxane); IR (KBr): *v* 3417, 4417 (NH), 3247, 3163 (NH_2), 3050, 2985 (CH), 1689 (C=O) $cm^{-1;}$ ^{1}H NMR (DMSO-d_6): δ 6.86–7.88 (m, 3H, Ar-H), 8.79, 9.07 (d, 2H, NH_2), 11.26 (s, 1H, NH), 12.28 (s, 1H, NH); ^{13}C NMR (DMSO-d_6): δ 112.9, 114.1, 122.2, 123.4, 130.6, 133.1, 141.3 (Ar-C), 162.2 (C=S), 178.7 (C=O) ppm; MS m/z (%): 299 (M^{+}, 14), 266 (46), 246 (45), 229 (65), 215 (500), 183 (46), 158 (32), 119 (40), 115 (77), 106 (100), 60 (43). Anal. Calcd for $C_9H_7BrN_4OS$ (299.15): C, 36.14; H, 2.36; N, 18.73. Found: C, 36.45; H, 2.08; N, 18.45%.

The Reaction of Thiosemicarbazone Derivative 3 with Hydrazonoyl Chlorides 4a-h and 8a-f

General procedure: To a stirred solution of bis-thiosemicarbazone derivative 3 (0.299 g, 1 mmol) and the appropriate hydrazonoyl chloride 4a-h or 8a-f (1 mmol) in dioxane (30 mL), was added trimethylamine (1 mL) and the mixture was refluxed for 4–6 h. The precipitated triethylamine hydrochloride was filtered off, and the filtrate was evaporated under reduced pressure. The residue was triturated with methanol. The solid product, so formed in each case, was collected by filtration, washed with water, dried, and crystallized from the dioxane solvent to afford the corresponding thiazole derivatives 7 or 11, respectively. The compounds 7a-h and 11a-f prepared are listed below together with their physical constants.

(3)-5-Bromo-3-((4-methyl-5-(2-phenylhydrazono)thiazol-2(5*H*)-ylidene)hydrazono)indolin-2-one (7a)

Red solid, 72% yield; mp. 298–299 °C; IR (KBr): *v* 3441, 3163 (2NH), 3062, 2938 (CH), 1689 (C=O) $cm^{-1;}$ ^{1}H NMR (DMSO-d_6): δ 2.15 (s, 3H, CH_3), 6.84–7.94 (m, 8H, Ar-H), 9.88 (s, 1H, NH), 10.73 (s, 1H, NH)ppm; ^{13}C NMR

(DMSO-d_6): δ 21 (CH_3), 103.2, 115.2, 119.3, 122.5, 125.6, 128.9, 129.4, 130.9, 132.3, 136.2, 137.1, 138.6, 142.3, 150.7 (Ar-C), 161.8 (C=O) ppm; MS m/z (%): 441 (M^+, 18), 413 (62), 405 (72), 397 (43), 357 (100), 344 (51), 326 (70), 317 (63), 290 (71), 264 (43), 168 (51), 131 (52), 114 (39), 57 (63), 49 (92). Anal. Calcd for $C_{18}H_{13}BrN_6OS$ (441.31): C, 48.99; H, 2.97; N, 19.04. Found: C, 49.16; H, 2.82; N, 18.86%.

(3)-5-Bromo-3-((5-(2-(4-chlorophenyl)hydrazono)-4-methylthiazol-2(5*H*)-ylidene) hydrazono)indolin-2-one (7b)

Red solid, 74% yield; mp. 260–261 °C; IR (KBr): *v* 3433, 3124 (2NH), 3060, 2930 (CH), 1689 (C=O) $cm^{-1;}$ ^{1}H NMR (DMSO-d_6): δ 2.14 (s, 3H, CH_3), 7.06–7.82 (m, 7H, Ar-H), 10.05 (s, 1H, NH), 10.72 (s, 1H, NH)ppm; MS m/z (%): 478 (M^++2, 24), 476 (M^++1, 24), 475 (M^+, 32), 454 (38), 449 (39), 372 (66), 347 (36), 328 (32), 299 (38), 284 (61), 257 (55), 224 (100), 172 (59), 101 (35). Anal. Calcd for $C_{18}H_{12}BrClN_6OS$ (475.75): C, 45.44; H, 2.54; N, 17.67. Found: C, 45.67; H, 2.34; N, 17.46%.

(3)-5-Bromo-3-((5-(2-(4-Bromophenyl)hydrazono)-4-methylthiazol-2(5*H*)-ylidene) hydrazono)indolin-2-one (7c)

Red solid, 75% yield; mp. 320–321 °C; IR (KBr): *v* 3433, 3150 (2NH), 3042, 2978 (CH), 1689 (C=O) $cm^{-1;}$ ^{1}H NMR (DMSO-d_6): δ 2.16 (s, 3H, CH_3), 7.10–7.94 (m, 7H, Ar-H), 8.75 (s, 1H, NH), 10.96 (s, 1H, NH); MS m/z (%): 517 (M^+, 24), 480 (19), 381 (33), 312 (39), 291 (52), 254 (53), 220 (95), 183 (62), 125 (51), 112 (100), 92 (61), 65 (48), 44 (56). Anal. Calcd for $C_{18}H_{12}Br_2N_6OS$ (517.92): C, 41.56; H, 2.33; N, 16.16. Found: C, 41.81; H, 2.17; N, 16.00%.

(3)-5-Bromo-3-((5-(2-(4-fluorophenyl)hydrazono)-4-methylthiazol-2(5*H*)-ylidene) Hydrazono)indolin-2-one (7d)

Red solid, 74% yield; mp. 247–249 °C; IR (KBr): *v* 3433, 3250 (2NH), 3040, 2924 (CH), 1658 (C=O) $cm^{-1;}$ ^{1}H NMR (DMSO-d_6): δ 2.14 (s, 3H, CH_3), 6.83–7.82 (m, 7H, Ar-H), 9.87 (s, 1H, NH), 10.65 (s, 1H, NH) ppm; MS m/z (%): 458 (M^+, 36), 427 (40), 314 (75), 303 (57), 294 (100), 263 (67), 212 (55), 144 (86), 54 (82). Anal. Calcd for $C_{18}H_{12}BrFN_6OS$ (458.31): C, 47.07; H, 2.63; N, 18.30. Found: C, 47.29; H, 2.39; N, 18.11%.

(3)-5-Bromo-3-((4-methyl-5-(2-(p-tolyl)hydrazono)thiazol-2(5*H*)-ylidene)hydrazono) indolin-2-one (7e)

Red solid, 67% yield; mp. 303–305 °C; IR (KBr): *v* 3433, 3288 (2NH), 3109, 2978 (CH), 1689 (C=O) $cm^{-1;}$ ^{1}H NMR (DMSO-d_6): δ 2.23 (s, 3H, CH_3), 2.40 (s, 3H, CH_3), 6.98–7.94 (m, 7H, Ar-H), 10.10 (s, 1H, NH), 10.37 (s, 1H, NH); MS m/z (%): 455 (M^+, 47), 443 (58), 411 (55), 397 (55), 369 (43), 347 (46), 321 (64), 295 (57), 265 (70), 229 (70), 172 (100), 150 (64), 98 (68), 49 (86). Anal. Calcd for $C_{19}H_{15}BrN_6OS$ (455.33): C, 50.12; H, 3.32; N, 18.46. Found: C, 50.36; H, 3.15; N, 18.28%.

(3)-5-Bromo-3-((5-(2-(4-methoxyphenyl)hydrazono)-4-methylthiazol-2(5*H*)-ylidene) hydrazono)indolin-2-one (7f)

Red solid, 78% yield; mp. 315–316 °C; IR (KBr): *v* 3410, 3170 (2NH), 3000, 2970 (CH), 1697 (C=O) $cm^{-1;}$ ^{1}H NMR (DMSO-d_6): δ 2.49 (s, 3H, CH_3), 3.56 (s, 3H, OCH_3), 6.78–7.81 (m, 7H, Ar-H), 8.40 (s, 1H, NH), 10.67 (s, 1H, NH); MS m/z (%): 471 (M^+, 63), 434 (42), 415 (68), 373 (69), 306 (34), 229 (54), 150 (98), 131 (61), 118 (38), 105 (100), 95 (55), 78 (67). Anal. Calcd for $C_{19}H_{15}BrN_6O_2S$ (471.33): C, 48.42; H, 3.21; N, 17.83. Found: C, 48.68; H, 3.04; N, 17.63%.

(3)-5-Bromo-3-((4-methyl-5-(2-(4-Nitrophenyl)hydrazono)thiazol-2(5*H*)-ylidene) hydrazono)indolin-2-one (7g)

Red solid, 70% yield; mp. 300–302 °C; IR (KBr): *v* 3402, 3194 (2NH), 3101, 2978 (CH), 1712 (C=O) $cm^{-1;}$ ^{1}H NMR (DMSO-d_6): δ 2.17 (s, 3H, CH_3), 7.04–7.82 (m, 7H, Ar-H), 9.92 (s, 1H, NH), 10.68 (s, 1H, NH)ppm; MS m/z (%): 486 (M^+, 18), 429 (40), 391 (24), 318 (20), 238 (74), 168 (39), 153 (38), 132 (38), 79 (38), 72 (100), 44 (33). Anal. Calcd for $C_{18}H_{12}BrN_7O_3S$ (486.30): C, 44.46; H, 2.49; N, 20.16. Found: C, 44.79; H, 2.30; N, 20.02%.

(3)-5-Bromo-3-((5-(2-(4-fluoro-3-methylphenyl)hydrazono)-4-methylthiazol-2(5*H*)-ylidene) hydrazono) indolin-2-one (7h)

Red solid, 76% yield; mp. 310–311 °C; IR (KBr): *v* 3441, 3201 (2NH), 2978, 2916 (CH), 1689 (C=O) $cm^{-1;}$ ^{1}H NMR (DMSO-d_6): δ 2.16 (s, 3H, CH_3), 2.24 (s, 3H, CH_3), 7.04–7.94 (m, 6H, Ar-H), 9.93 (s, 1H, NH), 10.77 (s, 1H, NH) ppm; ^{13}C NMR (DMSO-d_6): δ 24.8, 28.6 ($2CH_3$), 105.0, 115.2, 120.0, 120.6, 122.5, 125.5, 127.5, 128.8, 130.0, 131.6, 233.9, 136.4, 138.6, 148.5 (Ar-C), 161.0 (C=O) ppm; MS m/z (%): 473 (M^+, 29), 454 (91), 434 (74), 372 (63), 318 (29), 268 (36), 247 (60), 205 (56), 185 (53), 158 (36), 98 (94), 80 (100). Anal. Calcd for $C_{19}H_{14}BrFN_6OS$ (473.32): C, 48.21; H, 2.98; N, 17.76. Found: C, 48.48; H, 2.70; N, 17.44%.

5-Bromo-3-((−4-ethoxy-5-(2-phenylhydrazono)thiazol-2(5*H*)-ylidene)hydrazono)indolin-2-one (11a)

Orange solid, 74% yield; mp. 265–266 °C; IR (KBr): *v* 3430, 3348 (2NH), 3101, 2985 (CH), 1728 (OEt) $cm^{-1;}$ ^{1}H NMR (DMSO-d_6): δ 1.32–1.37 (m, 3H, CH_3), 4.37–4.42 (q, 2H, CH_2), 6.76–7.87 (m, 8H, Ar-H), 7.98 (s, 1H, NH), 10.75 (s, 1H, NH); MS m/z (%): 471 (M^+, 19), 424 (41), 418 (34), 375 (17), 339 (23), 325 (21), 298 (27), 283 (84), 234 (77), 219 (42), 188 (100), 181 (67), 159 (46), 143 (57). Anal. Calcd for $C_{19}H_{15}BrN_6O_2S$ (471.33): C, 48.42; H, 3.21; N, 17.83. Found: C, 48.61; H, 3.03; N, 17.66%.

5-Bromo-3-((5-(2-(4-chlorophenyl)hydrazono)-4-ethoxythiazol-2(5H)-ylidene)hydrazono) indolin-2-one (11b)

Orange solid, 74% yield; mp. 299–300 °C; IR (KBr): *v* 3441, 3350 (2NH), 3186, 2985 (CH), 1728 (OEt) $cm^{-1;}$ ^{1}H NMR (DMSO-d_6): δ 1.32–1.38 (m, 3H, CH_3), 4.38–4.45 (q, 2H, CH_2), 6.77–7.92 (m, 7H, Ar-H), 8.38 (s, 1H, NH), 10.76 (s, 1H, NH); ^{13}C NMR (DMSO-d_6): δ 33.1 (CH_3), 55.4 (CH_2), 115.3, 119.1, 122.5, 124.8, 126.0, 129.4, 131.6, 135.1, 136.0, 138.7, 139.5, 141.8151.0, 155.9 (Ar-C), 174.4 (C=O) ppm; MS m/z (%): 506 (M^+, 28), 482 (42), 465 (45), 492 (100), 401 (51), 363 (43), 344 (51), 305 (76), 222 (54), 184 (55), 77 (56), 61 (46), 53 (70), 41 (57). Anal. Calcd for $C_{19}H_{14}BrClN_6O_2S$ (505.77): C, 45.12; H, 2.79; N, 16.62. Found: C, 45.30; H, 2.68; N, 16.51%.

5-Bromo-3-((4-ethoxy-5-(2-(p-tolyl)hydrazono)thiazol-2(5*H*)-ylidene)hydrazono)indolin-2-one (11c)

Orange solid, 74% yield; mp. 290–291 °C; IR (KBr): *v* 3355, 3178 (2NH) 2985, 2908 (CH), 1720 (OEt) $cm^{-1;}$ ^{1}H NMR (DMSO-d_6): δ 1.32–1.37 (m, 3H, CH_3), 2.42 (s, 3H, CH_3), 4.38–4.45 (q, 2H, CH_2), 6.76–7.73 (m, 7H, Ar-H), 7.95 (s, 1H, NH), 10.74 (s, 1H, NH); MS m/z (%): 485 (M^+, 74), 478 (94), 462 (46), 437 (48), 381 (51), 343 (46), 303 (40), 286 (80), 245 (100), 236 (46), 182 (39), 159 (67), 121 (45), 100 (55), 62 (35). Anal. Calcd for $C_{20}H_{17}BrN_6O_2S$ (485.36): C, 49.49; H, 3.53; N, 17.32. Found: C, 49.62; H, 3.45; N, 17.06%.

5-Bromo-3-((4-ethoxy-5-(2-(4-nitrophenyl)hydrazono)thiazol-2(5*H*)-ylidene)hydrazono) indolin-2-one (11d)

Orange solid, 74% yield; mp. 262–263 °C; IR (KBr): *v* 3448, 3186 (2NH), 3078, 2916 (CH), 1735 (OC=O) $cm^{-1;}$ ^{1}H NMR (DMSO-d_6): δ 1.34–1.38 (m, 3H, CH_3), 4.40–4.47 (q, 2H, CH_2), 6.76–8.48 (m, 7H, Ar-H), 7.99 (s, 1H, NH), 10.81 (s, 1H, NH); ^{13}C NMR (DMSO-d_6): δ 33.1 (CH_3), 54.8 (CH_2), 115.5, 118.9, 122.6, 123.1125.6, 129.0, 131.0, 133.2, 135.4, 139.3, 141.2, 142.5, 150.9, 155.1 (Ar-C), 174.2 (C=O) ppm; MS m/z (%): 516 (M^+, 45), 453 (42), 388 (36), 333 (34), 296 (100), 273 (92), 256 (31), 225 (35), 210 (71), 134 (55), 108 (34), 44 (47). Anal. Calcd for $C_{19}H_{14}BrN_7O_4S$ (516.33): C, 44.20; H, 2.73; N, 18.99. Found: C, 44.34; H, 2.63; N, 18.81%.

Ethyl 4-(2-(2-((−5-bromo-2-oxoindolin-3-ylidene)hydrazono)-4-ethoxythiazol-5(2H)-ylidene)hydrazinyl) benzoate (11e)

Orange solid, 74% yield; mp. 249–250 °C; IR (KBr): *v* 3425, 3271 (2NH), 2978, 2931 (CH), 1720, 1700 (2OEt) $cm^{-1;}$ ^{1}H NMR (DMSO-d_6): δ 1.15–1.38 (m, 6H, $2CH_3$), 4.31–4.44 (q, 4H, $2CH_2$), 6.73–7.99 (m, 7H, Ar-H), 8.17 (s, 1H, NH), 10.75 (s, 1H, NH); MS m/z (%): 543 (M^+, 35), 533 (35), 493 (33), 453 (41), 400 (37), 369 (40), 350 (34), 317 (57), 287 (55), 256 (57), 202 (36), 196 (100), 163 (79), 94 (36), 71 (73), 58 (62). Anal. Calcd for $C_{22}H_{19}BrN_6O_4S$ (543.40): C, 48.63; H, 3.52; N, 15.47. Found: C, 48.82; H, 3.48; N, 15.29%.

5-Bromo-3-((4-ethoxy-5-(2-(4-fluoro-3-methylphenyl)hydrazono)thiazol-2(5H)-ylidene)hydrazono)indolin-2-one (11f)

Orange solid, 74% yield; mp. 296–297 °C; IR (KBr): *v* 3425, 3178 (2NH), 2978, 2924 (CH), 1728 (OEt) $cm^{-1;}$ ^{1}H NMR (DMSO-d_6): δ 1.32–1.38 (m, 3H, CH_3), 2.35 (s, 3H, CH_3), 4.39–4.46 (q, 2H, CH_2), 6.79–7.75 (m, 6H, Ar-H), 7.95 (s, 1H, NH), 10.78 (s, 2H, 2NH); MS m/z (%): 503 (M^+, 60), 454 (63), 426 (45), 409 (47), 376 (35), 324 (53), 302 (100), 298 (72), 264 (34), 208 (45), 167 (45), 147 (56), 63 (37). Anal. Calcd for $C_{20}H_{16}BrFN_6O_2S$ (503.02): C, 47.72; H, 3.20; N, 16.70;. Found: C, 48.00; H, 3.05; N, 16.53%.

Synthesis of Thiazole Derivatives 14a-e

General procedure: A mixture of thiosemicarbazone derivative 3 (0.299 g, 1 mmol) and the appropriate α-haloketones 12a-e (1 mmol) in ethanol (20 mL) was refluxed for 2–4 h. During the reaction, a precipitate was formed. The precipitate was collected by filtration, washed with ethanol, dried, and crystallized from EtOH to afford the corresponding thiazoles 14a-e.

5-Bromo-3-(2-(4-phenylthiazol-2-yl)hydrazono)indolin-2-one (14a) was synthesized according to the reported procedure[24]

Green solid, 70% yield; mp. 290°C (lit 285–287°C); IR (KBr): *v* 3425, 3209 (2NH), 3078, 2924 (CH), 1689 (C=O) $cm^{-1;}$ ^{1}H NMR (DMSO-d_6): δ 6.82–7.94 (m, 8H, Ar-H), 8.51 (s, 1H, thiazole-H5), 11.34 (s, 1H, NH), 13.35 (s, 1H, NH); MS m/z (%): 399 (M^+, 26), 378 (51), 339 (36), 328 (53), 319 (100), 304 (45), 256 (55), 238 (30), 201 (54), 188 (45), 139 (48), 120 (37), 104 (71), 48 (58). Anal. Calcd for $C_{17}H_{11}BrN_4OS$ (399.27): C, 51.14; H, 2.78; N, 14.03. Found: C, 51.44; H, 2.50; N, 13.70%.

5-Bromo-3-(2-(4-(4-chlorophenyl)thiazol-2-yl)hydrazono)indolin-2-one (14b)

Green solid, 73% yield; mp. 310 °C; IR (KBr): *v* 3433, 3209 (2NH), 3055, 2925 (CH), 1681 (C=O) $cm^{-1;}$ ^{1}H NMR (DMSO-d_6): δ 6.80–7.93 (m, 7H, Ar-H), 8.51 (s, 1H, thiazole-H5), 11.34 (s, 1H, NH), 13.31 (s, 1H, NH)ppm; MS m/z (%): 435 (M^+ +2, 38), 434 (M^+ +1, 38), 433 (M^+, 22), 408 (32), 387 (67), 362 (100), 352 (66), 309 (51), 283 (48), 203 (33), 185 (44), 164 (69), 102 (88), 74 (52), 52 (79), 47 (97). Anal. Calcd for $C_{17}H_{10}ClBrN_4OS$ (433.71): C, 47.08; H, 2.32; N, 12.92. Found: C, 47.36; H, 2.05; N, 12.63%.

5-Bromo-3-(2-(4-(4-Bromophenyl)thiazol-2-Yl)hydrazono)indolin-2-One (14c)

Green solid, 70% yield; mp. 312 °C; IR (KBr): *v* 3448, 3155 (2NH), 3055, 3016 (CH), 1689 (C=O) $cm^{-1;}$ ^{1}H NMR (DMSO-d_6): δ 6.79–7.86 (m, 7H, Ar-H), 8.50 (s, 1H, thiazole-H5), 11.34 (s, 1H, NH), 13.38 (s, 1H, NH); ^{13}C NMR (DMSO-d_6): δ 115.2, 116.9, 122.5, 125.0, 126.8, 129.2, 131.5, 133.4, 135.9, 138.1, 129.3, 132.5, 151.0, 160.2 (Ar-C), 172.2 (C=O) ppm; MS m/z (%): 478 (M^+, 32), 445 (46), 427 (57), 415 (44), 373 (95), 344 (60), 313 (60), 258 (65), 261 (60), 251 (92), 198 (100), 161 (30), 128 (41), 105 (48), 67 (81), 43 (53). Anal. Calcd for $C_{17}H_{10}Br_2N_4OS$ (478.16): C, 42.70; H, 2.11; N, 11.72. Found: C, 43.00; H, 1.80; N, 11.44%.

5-Bromo-3-(2-(4-(p-tolyl)thiazol-2-yl)hydrazono)indolin-2-one (14d)

Green solid, 76% yield; mp. 305 °C; IR (KBr): *v* 3448, 3155 (2NH), 3047, 2924 (CH), 1689 (C=O) $cm^{-1;}$ ^{1}H NMR (DMSO-d_6): δ 2.35 (s, 1H, CH_3), 6.79–7.80 (m, 7H, Ar-H), 8.52 (s, 1H, thiazole-H5), 11.34 (s, 1H, NH), 13.40 (s, 1H, NH)ppm; ^{13}C NMR (DMSO-d_6): δ 33.2 (CH_3), 115.2, 118.9, 119.3, 122.6, 125.2, 127.6, 129.8, 130.7, 131.6, 134.3, 136.0, 138.5, 143.2, 150.6 (Ar-C), 165.5 (C=O) ppm; MS m/z (%): 413 (M^+, 44), 343 (25), 317 (100), 280 (68), 260 (91), 245 (92), 217 (67), 205 (40), 198 (24), 71 (83). Anal. Calcd for $C_{18}H_{13}BrN_4OS$ (413.29): C, 52.31; H, 3.17; N, 13.56. Found: C, 52.60; H, 2.90; N, 13.25%.

5-Bromo-3-(2-(4-(4-nitrophenyl)thiazol-2-Yl)hydrazono)indolin-2-one (14e)

Green solid, 65% yield; mp. 325 °C; IR (KBr): *v* 3402, 3240 (2NH), 3124, 2931 (CH), 1689 (C=O) $cm^{-1;}$ ^{1}H NMR (DMSO-d_6): δ 6.86–8.19 (m, 7H, Ar-H), 8.22 (s, 1H, thiazole-H5), 11.31 (s, 1H, NH), 13.20 (s, 1H, NH); MS m/z (%): 444 (M^+, 22), 425 (31), 384 (74), 383 (100), 323 (34), 303 (56), 246 (59), 148 (20), 119 (36), 96 (26), 78 (43), 70 (34). Anal. Calcd for $C_{17}H_{10}BrN_5O_3S$ (444.26): C, 45.96; H, 2.27; N, 15.76. Found: C, 46.25; H, 2.00; N, 15.47%.

Assessment of Antimicrobial Activity

The antimicrobial effects of isatin derivatives were assessed against 2 bacterial strains, the Gram-negative *Escherichia coli* ATCC 25922 and the Gram-positive MRSA ATCC 43300. In addition, the anti-fungal activity was measured against *Candida albicans* ATCC 10231. The activity of tested compounds was measured using the agar well diffusion method according to the specifications of the Clinical and Laboratory Standards Institute.[25] Adjusted spectrophotometrically, 10^7CFU (Colony Forming Unit) of each microorganism were seed inoculated on Muller Hinton agar (MHA) plates for *E. coli* and *S. aureus*, or Sabouraud Dextrose Agar (SDA) for *C. Albicans* before a cork borer was used to punch wells (12 mm diameter) in the agar media. All isatin derivatives were dissolved to a concentration of 100 mg/mL in DMSO and then diluted in phosphate-buffered saline (pH7) to reach a final concentration of 1 mg/mL. Wells were filled with 100 µL of solution. DMSO (1% in phosphate-buffered saline) was used as a negative control, while chloramphenicol (for *E. coli* and *S. aureus*, 1 mg/mL) and nystatin (for *C. Albicans*, 1 mg/mL) were used as positive controls. MHA plates were incubated overnight at 37°C, whereas SDA plates were incubated for 48h at 25°C before measuring inhibition zone diameters.

Determination of MIC

The minimum inhibitory concentrations (MIC) of isatin derivatives that have shown antimicrobial activity were determined against the same isolates using the broth microdilution method as described in the CLSI guidelines.[25] In brief, solutions of isatin derivatives were serially diluted, in microtiter plates, using Mueller Hinton Broth, for *E. coli* and *S. aureus*, and Sabouraud dextrose broth for *C. Albicans*. The final concentrations of isatin derivatives in the solution ranged from 512 µg/mL to 0.5 µg/mL (512; 256; 128; 64; 32; 16; 8; 4; 2; 1; 0.5 µg/mL). After isatin derivatives were serial diluted, the specified microorganisms were inoculated so that inoculum density per well was 10^6 CFU/mL. Uninoculated wells were used as negative controls, while chloramphenicol (for *E. coli* and MRSA) and nystatin (for *C. Albicans*) at the same concentrations were used as positive controls. After 24h of incubation at 37°C for *E. coli* and *S. aureus* and 48h of incubation at 25°C for *C. Albicans*, MICs were reported as the lowest concentration able to inhibit visible microbial growth.

Effect on Biofilm Formation

The ability of isatin derivatives that have shown promising antibacterial activities to inhibit biofilm formation at half their MICs was conducted against the biofilm-forming strains MRSA ATCC 43300 and *E. coli* ATCC 25922 according to Plyuta et al.[26]

Freshly cultured slants were used to inoculate tubes containing double-strength nutrient broth (Difco, IL, USA) and incubated at 37°C overnight. Bacterial counts were adjusted to 1×10^8 CFU/mL and suspensions were centrifuged at 10000 rpm for 5 min. This inoculum was diluted 1:20 in fresh medium and dispensed as 100µL in 96-well flat-bottomed plates (Nunc™ Thermo Scientific™). Isatin derivatives were added (100µL; 0.5 MIC) and plates were incubated at 37°C for 24h. All experiments were conducted in triplicates. Each plate included uninoculated wells to serve as negative controls, wells containing only bacterial suspensions to be positive controls, and wells treated with chloramphenicol (0.5 MIC) to act as a standard. At the end of the incubation period, the suspensions were carefully aspirated and the formed biofilms were washed with 100µL of Phosphate Buffered Saline (NaCl: 137 mM; Na_2HPO_4: 10 mM, KH_2PO_4: 1.8 mM; pH 7.2) to remove free bacterial cells. Formed biofilms were stained with 100µL of 0.1% crystal violet solution and left at room temperature for 2 min. Excess dye was aspirated and wells were washed thoroughly with PBS. Glacial acetic acid (100µL, 33%) was used as a destaining solution to liberate the dye from biofilms into the solution, before absorbance of the stained biofilms was measured spectrophotometrically at 545 nm.

The percentage of biofilm inhibition was calculated using the following equation reported by Lemos[27] according to the following equation:

$$\text{Biofilm inhibition}(\%) = ((\text{OD}_{\text{control}} - \text{OD}_{\text{test}})/\text{OD}_{\text{control}}) \times 100$$

Effect on Preformed Biofilms

The biofilm disruption capacity was tested as described by Nostro.[28] Bacterial suspensions were prepared as above, dispensed as 100µL in 96-well flat-bottomed plates, and incubated at 37°C for 24h to allow for biofilm formation.

Unattached cells were removed by careful aspiration followed by washing with PBS, then solutions of isatin derivatives (100µL, 0.5 MIC) were added and incubation was done at 37°C for 48h. Staining and destaining were done as described above. Percentage disruption was calculated according to Lemos[27] using the equation:

$$\text{Biofilm disruption}(\%) = ((\text{OD}_{\text{control}} - \text{OD}_{\text{test}})/\text{OD}_{\text{control}}) \times 100$$

Docking Study of Target Compounds

Compounds were drawn, converted to 3D structures, and minimized using Avogadro.[29] Targets were downloaded from the protein data bank (https://www.rcsb.org/) under PDB codes 1JIJ for *S. aureus* TyrRS and 1VBM for *E. coli*. Ligands and protein preparation and docking with auto dock vina[30] were done using the virtual screening tool PyRx.[31] Docking was done in a grid box of 25^3 Å^3 centered on the co-crystalized ligand with an exhaustiveness of 16. Validation of the docking procedure was done as we reported earlier[32,33] through the redocking of the co-crystalized ligand and calculation of RMSD between docked and co-crystallized ligand using the DockRMSD server.[34]

Results and Discussion

Chemistry

Initially, the key thiosemicarbazone derivative 3 was prepared as previously reported[23] by condensation of 5-bromoisatin (1) with an equivalent amount of thiosemicarbazide 2 in acidic ethanol (Scheme 1).

A series of new thiazole derivatives 7a-h was synthesized from the reaction of 3 with a series of 2-oxo-*N*-arylpropanehydrazonoyl chlorides 4a-h in refluxing dioxane in presence of Et_3N (Scheme 2), presumably via the formation of intermediates 5 and 6. The chemical structures of all newly formed thiazoles 7a-h were confirmed with

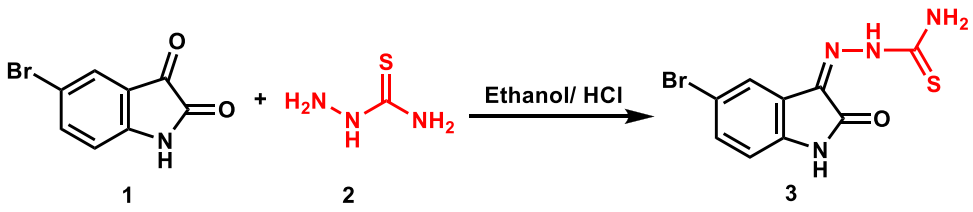

Scheme 1 Synthesis of thiosemicarbazone 3.

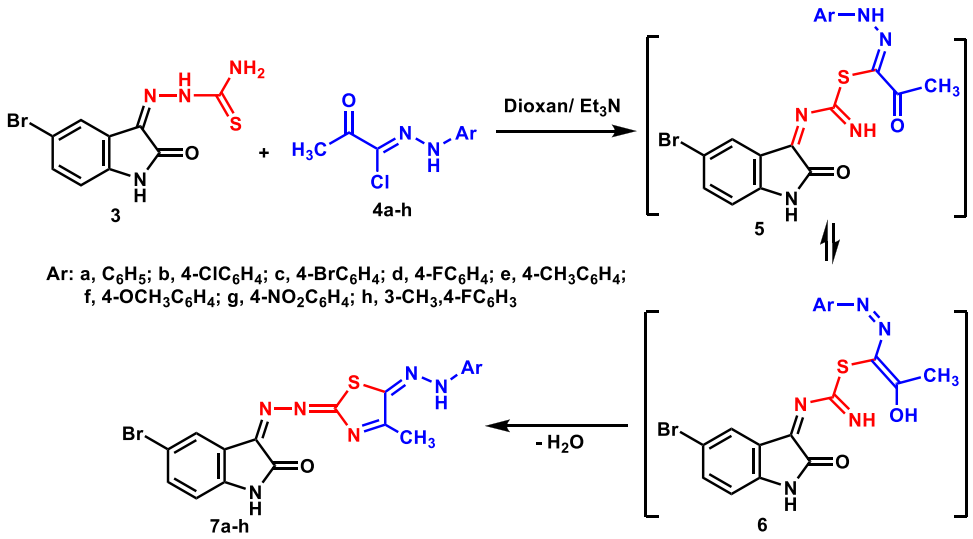

Scheme 2 Synthesis of isatin-decorated thiazole derivatives 7a-h.

spectral data and elemental analyses. The IR spectra of the newly formed thiazoles 7a-h revealed characteristic NH and Ar-*CH* stretches at ύ = 3410–3240, 3062–2940 cm^{-1}, respectively. Also, ^1H NMR of all thiazole derivatives 7a-h showed all expected signals for the suggested structures. For instance, compound 7a showed the characteristic singlets for the methyl group (CH_3) and the two -NH groups at 2.15, 9.88, and 10.73, respectively.

In a similar fashion, as shown in Scheme 3, compound 3 reacted with the respective 2-chloro-2-(2-phenylhydrazono) acetates 8a-f to form intermediate 9 which dehydrates and cyclizes to the corresponding 4-ethoxythiazole derivative 11a-f. The IR spectra revealed the absence of the ester C=O stretch as well as overlapped stretches for the two NH groups at ύ = 3430, 3348. The ^1H NMR of the thiazole derivatives 11a-f were consistent with the proposed structures. For example, the ^1H NMR spectrum of compound 11a had two singlet peaks at 7.98 and 10.75 for the two NH's along with the fingerprint triplet-quartet combination characteristic for the ethoxy group at δ 1.34 and 4.39, respectively.

The reactivity of precursor 3 towards various α-haloketones 12a-f was also explored. As a result, the reaction of 3 with α-haloketones 12a-e in refluxing ethanol led to the formation of a new series of thiazole derivatives 14a-e (Scheme 4), arguably via intermediate 13. ^1H NMR spectrum of compound 14a showed three singlet peaks at δ = 8.52, 11.34, and 13.35 representing thiazole-H5, isatin-NH, and hydrazone-NH, respectively.

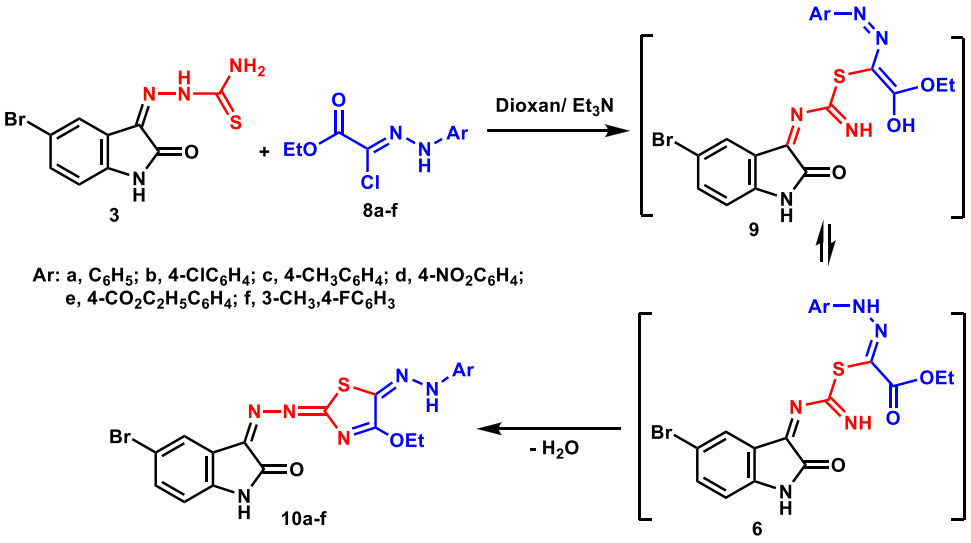

Scheme 3 Synthesis of ethoxy thiazole derivatives 11a-f.

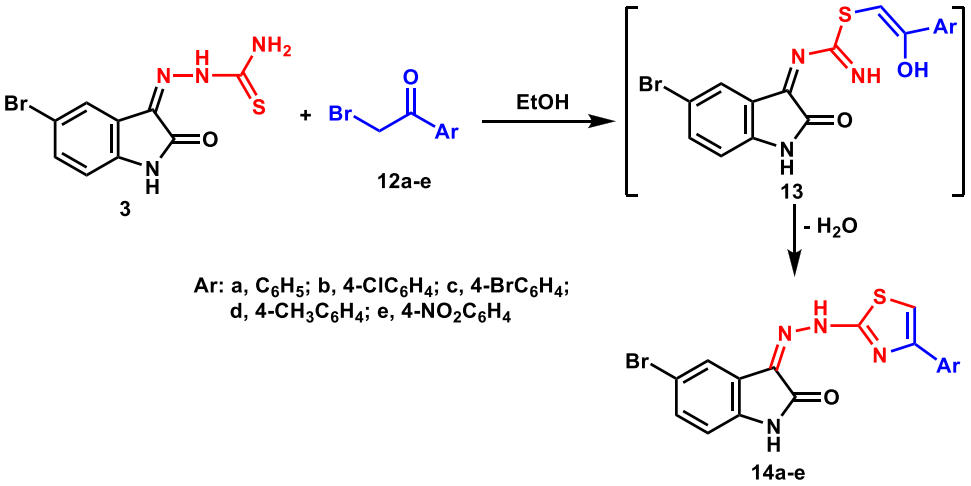

Scheme 4 Synthesis of thiazole derivatives 14a-e.

Assessment of Antimicrobial Activity and MIC Determination

Antimicrobial activities of the synthesized isatin-based thiazole derivatives were tested against *E. coli* (a common representative of Gram-negative pathogens), Methicillin-Resistant *Staphylococcus aureus* (MRSA), and *Candida albicans* using the cup-plate method. The compounds that have shown inhibition zones were further investigated for MIC using the broth microdilution method and their MIC values are listed in Tables 1–3.

When tested against *E. coli* (ATCC 25922), compounds 7b, 7d, and 14b displayed MICs eight times better than chloramphenicol, while compounds 14e and 14d had similar MICs to chloramphenicol (Table 1). The top three compounds (7b, 7d, and 14b) are 4-fluoro and 4-chloro derivatives which suggest the importance of electron-withdrawing groups. This is further supported by the moderate efficiency of 14e which is a 4-nitro derivative. Another important point is that the enlargement of the halogen from 4-chloro (7b or 14b) to 4-bromo (7c or 14c) will lead to loss of activity which suggests the importance of the size of the electron-withdrawing group used.

When tested against MRSA (ATCC 43300), compound 7f (4-methoxy) was the most potent with MIC one-eighth of that of chloramphenicol. In addition, both 11a (unsubstituted) and 11d (4-nitro) had equal MICs to that of chloramphenicol (Table 2). Meanwhile, compounds 11a and 11d had similar MICs as chloramphenicol. On another note, compounds 7h and 11f showed antifungal activities against *Candida albicans* (ATCC 10231) with MICs equal to that of the reference nystatin (Table 3). It is worth mentioning here that, both compounds have the same substitution pattern of 3-methyl-4-fluorophenyl moiety.

Effect on Biofilm Formation

Compounds with MIC values comparable to that of chloramphenicol were further screened, at 50% of their MIC values, as potential anti-biofilm formation agents (Tables 4 and 5). Compounds 11a (unsubstituted) and 11b (4-chloro) showed *ca*. 89 and 90% inhibition of biofilm formation by *E. coli* ATCC 25922, compared to 96% inhibition recorded for chloramphenicol. Compounds 11b (4-chloro) and 7d (4-fluro) showed *ca*. 66 and 71% inhibition of MRSA ATCC 43300

Table 1 MICs of Compounds Against *Escherichia coli* ATCC 25922

Compound	MIC (μg/mL)
3	128
7a	256
7b	4
7c	256
7d	4
7g	512
11a	512
11b	256
11c	256
14a	256
14b	4
14d	32
14e	32
Chloramphenicol	32

Table 2 MICs of Compounds Against MRSA ATCC 43300

Compound	MIC (μg/mL)
3	256
7a	64
7b	64
7d	128
7e	128
7f	1
7g	128
11a	8
11c	256
11d	8
11e	32
14a	256
14c	64
14d	128
14e	32
Chloramphenicol	8

Table 3 MICs of Compounds Against *Candida albicans* ATCC 10231

Compound	MIC (μg/mL)
7h	128
11f	128
Nystatin	128

biofilm formation, compared to 79% inhibition recorded for chloramphenicol. This suggests the superiority of small halogen substitution for this type of activity.

Effect on Preformed Biofilms

As shown in Tables 4 and 5 the screened compounds caused variable degrees of distortion of preformed *E. coli* and *S. aureus* biofilms with many showing comparable distortion percentages to those caused by chloramphenicol (76% for *E. coli* and 78% for *S. aureus*). Compound 14e (4-nitro) showed over 91% distortion of *E. coli* biofilms. Likewise, compounds 7a (unsubstituted), 7f (4-methoxy), and 11d (4-nitro) showed more than 91% distortion of *S. aureus* biofilms.

Table 4 Percent Biofilm Inhibition/Distortion Against *E. coli* ATCC 25922 Biofilms

Compound	Biofilm Inhibition (%± Standard Deviation)	Biofilm Distortion (%± Standard Deviation)
7a	46.79± 2.15	65.7± 0.55
7d	39.67± 5.52	64.31± 1.2
7f	12.17± 2.55	51.25± 2.19
11a	**89.22± 1.65**	78.84± 1.22
11b	**89.66± 0.20**	75.22± 0.45
11d	21.9± 3.41	62.74± 0.22
11e	30.71± 2.98	54.73± 0.21
14b	18.53± 0.19	67.67± 0.85
14d	66.71± 0.36	66.69± 1.26
14e	0± 1.15	**91.41± 0.46**
Chloramphenicol	95.98± 0.16	76.49± 1.21

Note: The bold figures represent the most potent inhibition/distortion values.

Table 5 Percent Biofilm Inhibition/Distortion Against MRSA ATCC 43300 Biofilms

Chemical Compound	Biofilm Inhibition (%± Standard Deviation)	Biofilm Distortion (%± Standard Deviation)
7a	11.6± 1.90	**91.47± 0.55**
7b	**65.6± 0.48**	81.37± 0.66
7d	22.34± 0.56	75.91± 0.44
7f	32.35± 2.10	**93.62± 0.42**
11a	14.21± 2.57	73.77± 1.44
11d	**70.59± 1.86**	**92.57± 0.86**
11e	44.00± 2.01	89.67± 0.48
14b	39.96± 1.94	75.33± 0.71
14d	19.43± 1.72	64.31± 1.91
14e	39.96± 1.10	77.63± 3.95
Chloramphenicol	79.07± 0.50	78.24± 1.09

Note: The bold figures represent the most potent inhibition/distortion values.

Molecular Docking Studies

Molecular docking is an important technique that could be used for virtual screening.[35] Docking is also used to investigate the potential binding modes of active compounds[36] which is our target here. In this study, all compounds were docked in the active sites of TyrRS of *E. coli* and *S. aureus* to investigate their possible binding modes. The crystal structures of *E. coli* TyrRS were downloaded from the protein data bank under the code 1VBM and co-crystalized with Tyr-AMS. Furthermore, the crystal structure of *S. aureus* TyrRS was downloaded under

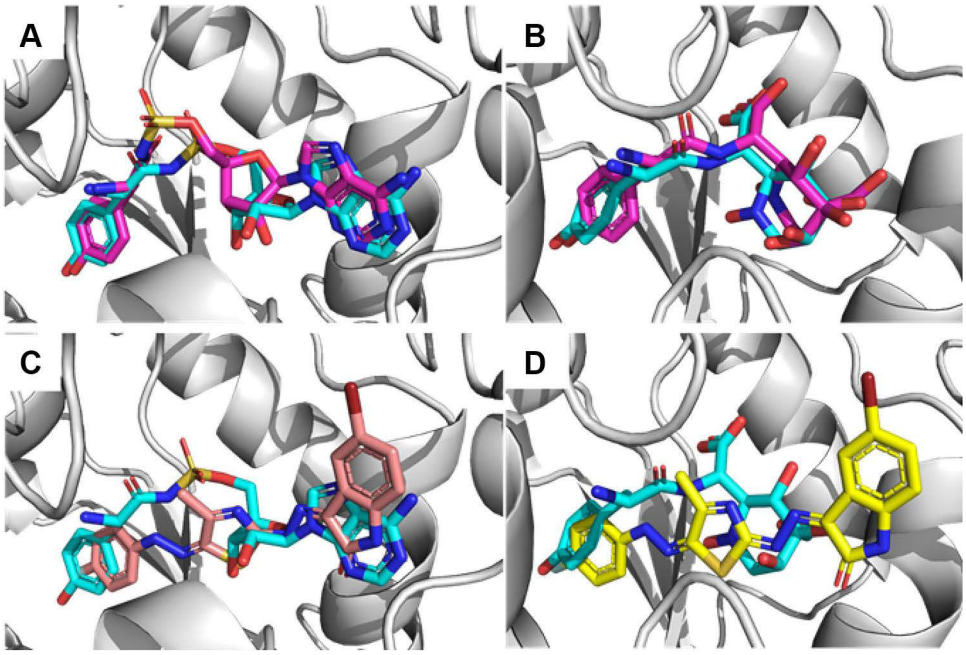

Figure 2 Docking results against bacterial TyrRS; (**A**) validation of docking procedure for *E. coli* TyrRS (1VBM) showing docked (pink) and co-crystalizes ligand (blue), (**B**) validation of docking procedure for *S. aureus* TyrRS (1JIJ), (**C**) docking of compound 7d (salmon) in the active site *E. coli* TyrRS (1VBM) overlapped with the co-crystallized ligand (blue), (**D**) docking of compound 7d (yellow) in the active site *S. aureus* TyrRS (1JIJ) overlapped with co-crystallized ligand (blue).

the code 1JIJ and co-crystalized with SB-239629 which is a known inhibitor with IC_{50} of 3 nM. Originally, the procedure was validated through the redocking of a co-crystalized ligand followed by calculating RMSD between docked and co-crystallized ligands. The RMSD was found to be 1.610 Å and 1.207 Å for 1VBM and 1JIJ, respectively (Figure 2A and B). These values are accepted (<2 Å) and suggest the validity of the docking procedure used. The binding modes of both co-crystallized ligands share similar interactions. These include a binding pocket for the hydroxyphenyl part of the tyrosine amino acid, the linker, the sugar-binding pocket, and the purine binding zone. In general, the docking scores showed better binding for compounds 7 and 11 compared to compound 14. Some of the tested compounds showed docking scores better than the co-crystalized ligands (Table 6). Docking poses of the tested compounds show binding modes similar to the co-crystalized ligand as it was initially designed. Figure 2C and D show the similar binding modes of a representative example of our compounds 7d with TyrRS of *E. coli* and *S. aureus*. The isatin ring is found to be docked in the purine binding pocket, while the thiazole ring of compounds 7, 11, and 14 along with the hydrazine moiety overlaps with the sugar part and the linker of the co-crystalized ligands. Finally, the terminal phenyl ring overlaps with the phenyl part of the tyrosine amino acid. This interesting binding mode would require further investigation. However, it provides a clearer view of plausible interaction modes between the newly synthesized compounds and this important target. A further validation for our molecular docking study using some in vitro methods was planned. Unfortunately, we were unable to express the TyrRS proteins in the laboratory due to their commercial unavailability of the TyrRS assay kits.

Conclusions

This study overlays the design and synthesis of isatin-decorated thiazole derivatives. In-vitro screening of the newly synthesized compounds for their antimicrobial activity showed promising results against both *E. coli* and MRSA with anti-biofilm formation activity. Compound 7f, the most potent antimicrobial compound in this study, showed a MIC value eight-fold better than chloramphenicol against MRSA. In addition, compounds 7h and 11f showed antifungal activities against *C. Albicans*. Several compounds showed inhibition and/or distortion of biofilm formation by *E. coli*. and *S. aureus*.

Table 6 Docking Scores of Compounds Against *S. aureus* TyrRS and *E. coli* TyrRS

Ligand	1JIJ	1VBM
	***S. aureus* TyrRS**	***E. coli* TyrRS**
3	−7.9	−8.6
7a	−10.2	−10.7
7b	−10	−11.1
7c	−9.9	−10.8
7d	−10.6	−11.2
7e	−10.4	−11.4
7f	−9.9	−10.8
7g	−10.4	−11.2
7h	−10.5	−10.4
11a	−9.9	−10.4
11b	−9.9	−10.8
11c	−10.2	−11
11d	−10.1	−11
11e	−9.6	−9.5
11f	−10.7	−11.1
14a	−9.5	−9.4
14b	−9.4	−9.9
14c	−9.3	−9.7
14d	−9.4	−10
14e	−9.6	−10
Co-crystalized ligand	−8.4 (SB-239629)	−10.6 (Tyr-AMS)

Molecular docking studies suggested the potential binding of the synthesized compounds with *S. aureus* and *E. coli* TyrRS like the binding modes of co-crystalized ligands. Exploring the full scope of the novel isatin-based thiazole derivatives as promising antibacterial prototypes, against potential target enzymes, is currently under further investigation (Supplementary Materials).

Acknowledgment

The authors are indebted to the generous funding provided by the deanship of scientific research, Imam Mohammad Ibn Saud Islamic University, Saudi Arabia, Research Group no. RG-21-09-77.

Disclosure

The authors report no conflicts of interest in this work.

References

1. Dhingra S, Rahman NAA, Peile E, et al. Microbial Resistance Movements: An Overview of Global Public Health Threats Posed by Antimicrobial Resistance, and How Best to Counter. *Frontiers in Public Health*. 2020;8:Article 535668. doi:10.3389/fpubh.2020.535668.

2. de Kraker MEA, Stewardson AJ, Harbarth S. Will 10 million people die a year due to antimicrobial resistance by 2050? *PLoS Med*. 2016;13(11): e1002184. doi:10.1371/journal.pmed.1002184
3. Cabrera R, Fernandez-Barat L, Motos A, et al. Molecular characterization of methicillin-resistant Staphylococcus aureus clinical strains from the endotracheal tubes of patients with nosocomial pneumonia. *Antimicrob Resist Infect Control*. 2020;9:359.
4. Qiu XY, Janson CA, Smith WW, et al. Crystal structure of Staphylococcus aureus tyrosyl-tRNA synthetase in complex with a class of potent and specific inhibitors. *Protein Sci*. 2001;10:2008–2016. doi:10.1110/ps.18001
5. Kobayashi T, Takimura T, Sekine R, et al. Structural snapshots of the KMSKS loop rearrangement for amino acid activation by bacterial tyrosyl-tRNA synthetase. *J Mol Biol*. 2005;354:739.
6. Hudson IRB. The efficacy of intranasal mupirocin in the prevention of staphylococcal infections - a review of recent experience. *J Hosp Infect*. 1994;27(2):81–98. doi:10.1016/0195-6701(94)90001-9
7. Brick P, Blow DM. Crystal-structure of a deletion mutant of a tyrosyl-transfer RNA-synthetase complexed with tyrosine. *J Mol Biol*. 1987;194 (2):287–297. doi:10.1016/0022-2836(87)90376-7
8. Winter G, Fersht AR, Wilkinson AJ, Zoller M, Smith M. Redesigning enzyme structure by site-directed mutagenesis - tyrosyl transfer-RNA synthetase and ATP binding. *Nature*. 1982;299(5885):756–758. doi:10.1038/299756a0
9. Zhang KY, Li X, Yu C, Wang Y. Promising therapeutic strategies against microbial biofilm challenges. *Front Cell Infect Microbiol*. 2020;10 doi:10.3389/fcimb.2020.00359
10. Lu L, Hu W, Tian ZR, et al. Developing natural products as potential anti-biofilm agents. *Chin Med*. 2019;14(1). doi:10.1186/s13020-019-0232-2
11. Mahmoud HK, Kassab RM, Gomha SM. Synthesis and characterization of some novel bis-thiazoles. *J Heterocycl Chem*. 2019;56(11):3157–3163. doi:10.1002/jhet.3717
12. Kassab RM, Gomha SM, Al-Hussain SA, et al. Synthesis and in-silico simulation of some new bis-thiazole derivatives and their preliminary antimicrobial profile: investigation of hydrazonoyl chloride addition to hydroxy-functionalized bis-carbazones. *Arab J Chem*. 2021;14(11):103396. doi:10.1016/J.ARABJC.2021.103396
13. Elgiushy HR, Abou-Taleb NA, Holz GG, et al. Synthesis, in vitro biological investigation, and molecular dynamics simulations of thiazolopyrimidine based compounds as corticotrophin releasing factor receptor-1 antagonists. *Bioorg Chem*. 2021;114:e105079.
14. Elrazaz EZ, Serya RAT, Ismail NSM, Albohy A, Abou El Ella DA, Abouzid KAM. Discovery of potent thieno[2,3-d]pyrimidine VEGFR-2 inhibitors: design, synthesis and enzyme inhibitory evaluation supported by molecular dynamics simulations. *Bioorg Chem*. 2021;113:e105019. doi:10.1016/j.bioorg.2021.105019
15. Kassab RM, Khalil FSAM, Abbas AA. Synthesis and antimicrobial activities of some new bis(Schiff Bases) and their triazole-based lariat macrocycles. *Polycycl Aromat Compd*. 2020;1–16. doi:10.1080/10406638.2020.1852272
16. West AC, Johnstone RW. New and emerging HDAC inhibitors for cancer treatment. *J Clin Invest*. 2014;124(1):30–39. doi:10.1172/JCI69738
17. Supuran CT, Winum JY. Carbonic anhydrase IX inhibitors in cancer therapy: an update. *Future Med Chem*. 2015;7(11):1407–1414. doi:10.4155/fmc.15.71
18. El-Azab AS, Al-Dhfyan A, Abdel-Aziz AAM, et al. Synthesis, anticancer and apoptosis-inducing activities of quinazoline–isatin conjugates: epidermal growth factor receptor-tyrosine kinase assay and molecular docking studies. *J Enzyme Inhib Med Chem*. 2017;32(1):935–944. doi:10.1080/14756366.2017.1344981
19. Vindya NG, Sharma N, Yadav M, Ethiraj KR. Tubulins - the target for anticancer therapy: ingenta connect. *Curr Top Med Chem*. 2015;15(1):73–82. doi:10.2174/1568026615666150112115805
20. Varun V, Sonam S, Kakkar R. Isatin and its derivatives: a survey of recent syntheses, reactions, and applications. *MedChemComm*. 2019;10(3):351. doi:10.1039/C8MD00585K
21. El-Abadelah MM, Hussein AQ, Thaher BA, A. Thaher B. Heterocycles from nitrile imines. Part IV. Chiral 4.5-dihydro-1,2,4-triazin-6-ones. *Heterocycles*. 1991;32:1879–1895. doi:10.3987/COM-90-5637
22. Matiichuk VS, Potopnyk MA, Obushak ND, Molecular design of pyrazolo[3,4-d]pyridazines. *Russ J Org Chem*. 2008;44(9):1352–1361. doi:10.1134/S1070428008090182
23. Singh AK, Shukla SK, Ahamad I, Quraishi MA. Solvent-Free microwave-assisted synthesis of 1H-Indole-2,3-dione derivatives. *J Heterocycl Chem*. 2009;46:571–574.
24. Eldehna WM, Al-Wabli RI, Almutairi MS, et al. Synthesis and biological evaluation of certain hydrazonoindolin-2-one derivatives as new potent anti-proliferative agents. *J Enzym Inhib Med Chem*. 2018;33(1):867–878. doi:10.1080/14756366.2018.1462802
25. CLSI. Performance standards for antimicrobial susceptibility testing. Twenty-Fourth informational supplement. Wayne, PA: Clinical and Laboratory Standards Institute, 2015.
26. Plyuta V, Zaitseva J, Lobakova E, Zagoskina N, Kuznetsov A, Khmel I. Effect of plant phenolic compounds on biofilm formation by Pseudomonas aeruginosa. *Apmis*. 2013;121:1073–1081. doi:10.1111/apm.12083
27. Lemos ASO, Campos LM, Melo L, et al. Antibacterial and antibiofilm activities of psychorubrin, a pyranonaphthoquinone isolated from Mitracarpus frigidus (Rubiaceae). *Front Microbiol*. 2018;9:724. doi:10.3389/fmicb.2018.00724
28. Nostro A, Roccaro AS, Bisignano G, et al. Effects of oregano, carvacrol and thymol on Staphylococcus aureus and Staphylococcus epidermidis biofilms. *J Med Microbiol*. 2007;56(4):519–523. doi:10.1099/jmm.0.46804-0
29. Hanwell MD, Curtis DE, Lonie DC, Vandermeersch T, Zurek E, Hutchison GR. Avogadro: an advanced semantic chemical editor, visualization, and analysis platform. *J Cheminform*. 2012;4(1). doi:10.1186/1758-2946-4-17
30. Trott O, Olson AJ. Software news and update AutoDock vina: improving the speed and accuracy of docking with a new scoring function, efficient optimization, and multithreading. *J Comput Chem*. 2010;31(2):455–461. doi:10.1002/jcc.21334
31. Dallakyan S, Olson AJ. Small-molecule library screening by docking with PyRx. *Chem Biol Methods Protoc*. 2015;1263:243–250. doi:10.1007/978-1-4939-2269-7_19
32. Ebada SS, Al-Jawabri NA, Youssef FS, et al. In vivo antiulcer activity, phytochemical exploration, and molecular modelling of the polyphenolic-rich fraction of Crepis sancta extract. *Inflammopharmacology*. 2020;28(1):321–331. doi:10.1007/s10787-019-00637-x
33. Ebada SS, Al-Jawabri NA, Youssef FS, et al. Anti-inflammatory, antiallergic and COVID-19 protease inhibitory activities of phytochemicals from the Jordanian hawksbeard: identification, structure-activity relationships, molecular modeling and impact on its folk medicinal uses. *Rsc Adv*. 2020;10(62):38128–38141. doi:10.1039/d0ra04876c

34. Bell EW, Zhang Y. DockRMSD: an open-source tool for atom mapping and RMSD calculation of symmetric molecules through graph isomorphism. *J Cheminform*. 2019;11(1). doi:10.1186/s13321-019-0362-7
35. Zahran EM, Albohy A, Khalil A, et al. Bioactivity potential of marine natural products from scleractinia-associated microbes and in silico anti-SARS-COV-2 evaluation. *Mar Drugs*. 2020;18(12):645. doi:10.3390/md18120645
36. Said MA, Albohy A, Abdelrahman MA, Ibrahim HS. Importance of glutamine 189 flexibility in SARS-CoV-2 main protease: lesson learned from in silico virtual screening of ChEMBL database and molecular dynamics. *Eur J Pharm Sci*. 2021;160:e105744. doi:10.1016/j.ejps.2021.105744